GLOBAL PHASE PORTRAITS OF THE KEY PITCHFORK BIFURCATION

SHIMIN LI[1] AND JAUME LLIBRE[2]

ABSTRACT. This paper deals with the following quadratic polynomial differential systems

$$\frac{dx}{dt} = y^2 - y - x, \qquad \frac{dy}{dt} = x^2 - \mu x - y,$$

with parameter $\mu \in \mathbb{R}$, which is the key example of [30] for studying the pitchfork bifurcation of a singular point. We classify the global phase portraits in the Poincaré disc of these systems when μ varies.

1. INTRODUCTION AND STATEMENT OF THE MAIN RESULTS

Global phase portraits are an invaluable tool in studying the long dynamical behaviour of differential systems. They reveals information such as whether an attractor, a repellor or a limit cycle is present for a given parameter value. Hence the global phase portraits analysis is the one of most important problems in the qualitative theory of differential systems.

The possibilities of topological distinct phase portraits for a general polynomial differential system are huge, it is expected that the quadratic polynomial differential systems have more than 2000 topological distinct phase portraits. Most of known results about global phase portraits of differential systems are mainly deal with special differential systems, see [1, 2, 3, 4, 6, 9, 11, 18, 27, 29, 31] for quadratic polynomial differential systems, see [5, 7, 10, 13, 14, 33, 34] for cubic polynomial differential systems, see [8, 25, 24, 26] for quartic polynomial differential systems, see [12, 15, 16, 17] for Liénard differential systems, see [22, 23, 28] for Hamiltonian differential systems. In [20] the authors introduce how to use the computer program $P4$ for drawing phase portraits in a Poincaré disc.

In a recent paper [30] Rajapakse and Smale considered the following quadratic polynomial differential systems

$$(1) \qquad \frac{dx}{dt} = y^2 - y - x, \qquad \frac{dy}{dt} = x^2 - \mu x - y,$$

as a key example to describe the pitchfork bifurcation, where $\mu \in \mathbb{R}$. They showed that symmetry is a dispensable condition for the existence of pitchfork bifurcation.

Let $\mathcal{X}_1$ and $\mathcal{X}_2$ be two vector fields defined on open subsets Δ_1 and Δ_2 of $\mathbb{R}^2$, respectively. We say that two vector fields $\mathcal{X}_1$ and $\mathcal{X}_2$ are *topologically equivalent*

1

when there exists a homeomorphism $h : \Delta_1 \to \Delta_2$ which sends orbits of $\mathcal{X}_1$ to orbits of $\mathcal{X}_2$ preserving or reversing the orientation.

In this paper we provide the topological classification of the phase portraits of systems (1) in the Poincaré disc.
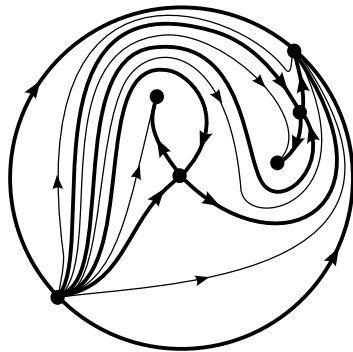
Theorem 1. *The global phase portrait of a differential system* (1) *is topologically equivalent to Figure* 1.1 *if* $\mu \leqslant 1$, *Figures* 1.2 *if* $1 < \mu < \mu^*$, *Figure* 1.3 *if* $\mu > \mu^*$ *and Figure* 1.4 *if* $\mu = \mu^*$, *where* $\mu^* \in (10.4722, 10.4723)$.
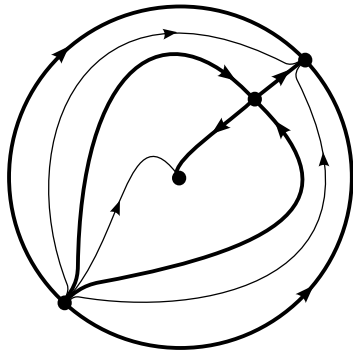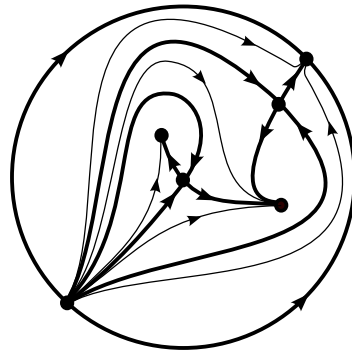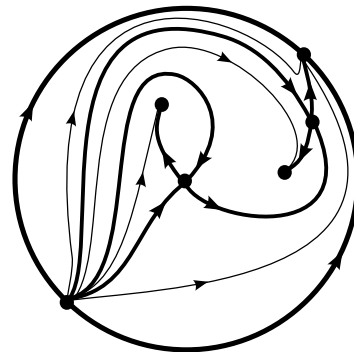

1.1 $S = 10, R = 3$ 1.2 $S = 16, R = 5$

1.3 $S = 16, R = 5$ 1.4 $S = 15, R = 4$

FIGURE 1. Topological phase portraits of differential systems (1). S and R denote the number of separatricies and canonical regions, respectively.

Note from Figure 1 that the pitchfork bifurcation at the origin of coordinates takes place at $\mu = 1$, where the stable node bifurcates into two stable foci and one saddle.

The layout of this paper is as follows. In section 2 we analyze the equilibria of systems (1) in the Poincaré compactification. In section 3 we prove Theorem 1.

2. Poincaré compactification

2.1. Poincaré compactification.

For a given polynomial differential system

$$(2) \qquad \frac{dx}{dt} = P(x,y), \qquad \frac{dy}{dt} = Q(x,y),$$

of degree $d = \max\{\deg(P), \deg(Q)\}$. Let $\mathcal{X} = (P, Q)$ be the vector field associated system (2).

We call $\mathbb{S}^2 = \{\mathbf{s} = (s_1, s_2, s_3) \in \mathbb{R}^3 : s_1^2 + s_2^2 + s_3^2 = 1\}$ the *Poincaré sphere*. The *Poincaré compactified vector field $p(\mathcal{X})$ corresponding to $\mathcal{X}$* is an analytic vector field induced on $\mathbb{S}^2$ as follows, for more details see Chapter 5 of [21].

First we take $\mathbb{R}^2$ as the plane in $\mathbb{R}^3$ defined by $(x, y, 1) \in \mathbb{R}^3$, and then project each point $(x, y, 1)$ in two points of the Poincaré sphere $\mathbb{S}^2$ using the straight line through $(x, y, 1)$ and the origin $(0, 0, 0)$. It is obvious that the equator $\mathbb{S}^1 = \{\mathbf{s} \in \mathbb{S}^2, s_3 = 0\}$ corresponds to the infinity of $\mathbb{R}^2$. So we have two copies of the vector field $\mathcal{X}$ on the Poincaré sphere $\mathbb{S}^2$, one in the open northern hemisphere $\mathbb{S}^- = \{\mathbf{s} \in \mathbb{S}^2 : s_3 > 0\}$, and the other in the open southern hemisphere $\mathbb{S}^+ = \{\mathbf{s} \in \mathbb{S}^2 : s_3 < 0\}$. This vector field on $\mathbb{S}^2 \setminus \mathbb{S}^1$ can be extended to a vector field $p(\mathcal{X})$ defined in the whole $\mathbb{S}^2$ multiplying it by s_3^d.

For studying the Poincaré sphere we use the following six local charts

$$(3) \qquad U_i = \{\mathbf{s} \in \mathbb{S}^2 : s_i > 0\}, \ V_i = \{\mathbf{s} \in \mathbb{S}^2 : s_i < 0\},$$

for $i = 1, 2, 3$.

The expression of $p(\mathcal{X})$ in the local charts U_1 and V_1 are given by

$$(4) \qquad \frac{du}{dt} = v^d \left[-uP\left(\frac{u}{v}, \frac{1}{v}\right) - uQ\left(\frac{u}{v}, \frac{1}{v}\right) \right], \qquad \frac{dv}{dt} = -v^{d+1} Q\left(\frac{u}{v}, \frac{1}{v}\right);$$

with $v > 0$ and $v < 0$, respectively.

The expression of $p(\mathcal{X})$ in the local charts U_2 and V_2 are given by

$$(5) \qquad \frac{du}{dt} = v^d \left[-uP\left(\frac{1}{v}, \frac{u}{v}\right) + Q\left(\frac{1}{v}, \frac{u}{v}\right) \right], \qquad \frac{dv}{dt} = -v^{d+1} P\left(\frac{1}{v}, \frac{u}{v}\right);$$

with $v > 0$ and $v < 0$, respectively.

The expression of $p(\mathcal{X})$ in the local charts U_3 and V_3 are just

$$(6) \qquad \frac{du}{dt} = P(u, v), \quad \frac{dv}{dt} = Q(u, v).$$

For studying the phase portrait of a differential system (2), we just need to study its Poincaré compactification $p(\mathcal{X})$ restricted to the closed northern hemisphere. We do the orthogonal projection $\pi(s_1, s_2, s_3) = (s_1, s_2)$ of the closed northern hemisphere onto the Poincaré disc $\mathbb{D}^2 = \{s_1^2 + s_2^2 \leqslant 1\}$ for drawing the phase portrait.

It is obvious that the finite equilibria of system (2) are the equilibria in the interior of $\mathbb{D}^2$, and they can be studied using U_3. The infinite equilibria of systems (2) are the equilibria of $p(\mathcal{X})$ in the boundary of $\mathbb{D}^2$. Note that for studying the infinite equilibria it suffices to look the ones at the local charts $U_1|_{v=0}$ and $V_1|_{v=0}$, and at the origin of the local charts U_2 and V_2.

2.2. In charts U_1 and V_1. Doing the change of variables $x = \dfrac{1}{v}, y = \dfrac{u}{v}$, systems (1) become

$$\frac{du}{dt} = 1 - v - u^3 + \mu u^2 v, \qquad \frac{dv}{dt} = v^2(v - u^2 + \mu uv).$$

Let $v = 0$, then we obtain the unique infinite equilibrium $(1, 0)$ in the chart U_1, which is a stable node. Since the degree of systems (1) is 2, so we can deduce that there is also a unique unstable node infinite equilibrium $(1, 0)$ in chart V_1 by symmetry.

2.3. In charts U_2 and V_2. Doing the change of variables $x = \dfrac{u}{v}, y = \dfrac{1}{v}$, systems (1) become

$$(7) \qquad \frac{du}{dt} = 1 - \mu v - u^3 + u^2 v, \qquad \frac{dv}{dt} = v(v - u^2 + uv).$$

Therefore the origin of U_2 and V_2 are not equilibria.

2.4. In charts U_3 and V_3. In order to determine the number of finite equilibrium of systems (1), we introduce the following result, see for example [32].

Lemma 2. *For a general quartic polynomial*

$$(8) \qquad a_0 x^4 + a_1 x^3 + a_2 x^2 + a_3 x + a_4, \quad (a_0 \neq 0).$$

We define the following parameters:

$$
\begin{aligned}
& E = 8a_0^2 a_3 + a_1^3 - 4a_0 a_1 a_2, \\
& D_2 = 3a_1^2 - 8a_0 a_2, \\
& D_3 = 16a_0^2 a_2 a_4 - 18a_0^2 a_3^2 - a_0 a_2^3 + 14a_0 a_1 a_2 a_3 - 6a_0 a_1^2 a_4 + a_1^2 a_2^2 - 3a_1^3 a_3, \\
(9) \quad & D_4 = 256a_0^3 a_4^3 - 27a_0^2 a_3^4 - 192a_0^2 a_1 a_3 a_4^2 - 27a_1^4 a_4^2 - 6a_0 a_1^2 a_3^2 a_4 + a_1^2 a_2^2 a_3^2 \\
& \qquad - 4a_0 a_2^3 a_3^2 + 18a_1^3 a_2 a_3 a_4 + 144a_0 a_1^2 a_2 a_4^2 - 80a_0 a_1 a_2^2 a_3 a_4 + 18a_0 a_1 a_2 a_3^3 \\
& \qquad - 4a_1^2 a_2^3 a_4 - 4a_1^3 a_3^3 + 16a_0 a_2^4 a_4 - 128a_0^2 a_2^2 a_4^2 + 144a_0^2 a_2 a_3^2 a_4.
\end{aligned}
$$

The following statements hold.

  (i) *If $D_4 > 0, D_3 > 0, D_2 > 0$, then (8) has four simple real zeros.*
  (ii) *If $D_4 < 0$, then (8) has two simple real zeros.*
  (iii) *If $D_4 = 0, D_3 = 0, D_2 > 0, E \neq 0$, then (8) has a simple zero and a triple zero.*

The finite equilibria of systems (1) must satisfy the following quartic polynomial

$$(10) \qquad f(y) = y(\mu - 1 - (\mu - 1)y - 2y^2 + y^3).$$

By direct computation we obtain

$$
\begin{aligned}
(11) \quad & E = -8, \quad D_2 = 4(1 + 2\mu), \quad D_3 = (\mu - 1)^3(4\mu^2 + 5\mu + 23), \\
& D_4 = 2(\mu - 1)(2\mu^2 + 3\mu + 7).
\end{aligned}
$$

If $\mu < 1$, then $D_4 < 0$. Therefore systems (1) have two simple finite equilibria $E_1 = (0,0)$ and E_2.

If $\mu = 1$, then $D_2 > 0$ and $D_3 = D_4 = 0$. Hence systems (1) have a simple finite equilibrium $E_1 = (0,0)$ and a triple finite equilibrium E_2.

If $\mu > 1$, then D_2, D_3 and D_4 are positive. So systems (1) have four simple finite equilibria $E_i, i = 1, 2, 3, 4$.

We state the well known Bendixson's Theorem as follows, see for instance Theorem 7.10 of [21].

Theorem 3 (Bendixson's Theorem). *Assume that the divergence function of differential system has constant sign in a simply connected region $\mathcal{R}$, and is not identically zero on any subregion of $\mathcal{R}$. Then differential system does not have a periodic orbit which lies entirely in $\mathcal{R}$.*

According to Bendixson's Theorem, we can obtain a preliminary result for systems (1).

Proposition 4. *Systems* (1) *have no periodic orbits, no homoclinic loops as the one of Figure 2.1.*

$$2.1 \quad \mu \in \mathbb{R} \qquad\qquad 2.2 \quad \mu > 1$$

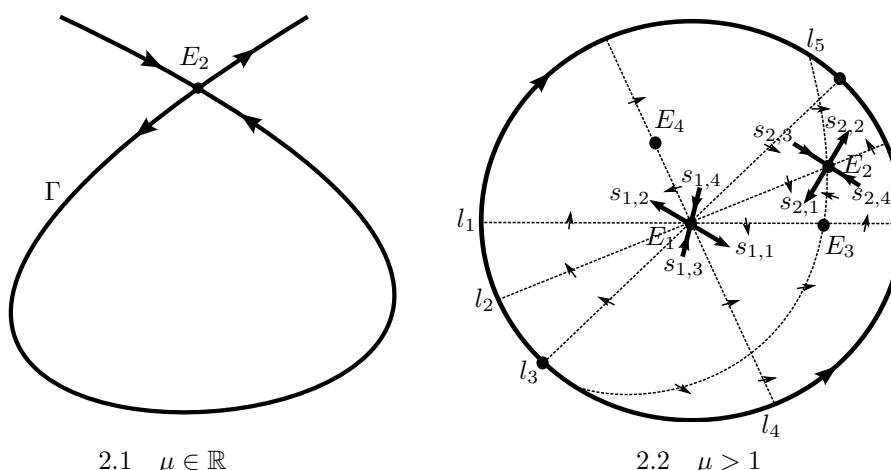FIGURE 2. 2.1. The homoclinic loop of the saddle E_2. 2.2. Local dynamics of the finite equilibria of systems (1) for $\mu > 1$. l_1, l_2, l_4 are the straight lines through the equilibria E_1 and E_3, E_2, E_4, respectively. l_3 is the straight line $y = x$. l_5 is the straight line through equilibria E_2 and E_3.

Proof. Since the divergence of systems (1) is -2, it follows that these systems have no periodic orbits by Theorem 3. Assume that systems (1) have a homoclinic loop Γ containing equilibrium E_2, see Figure 2.1. From Green's formula we have

$$(12) \qquad \int_\Gamma P dy - Q dx = \iint_{int(\Gamma)} \left(\frac{\partial P}{\partial x} + \frac{\partial Q}{\partial y} \right) dx dy.$$

Note that Γ is an orbit of systems (1), $Pdy - Qdx = 0$ holds everywhere along Γ. Hence the left side of (12) is zero. Recall that the divergence of systems (1) is -2, so the right side of (12) negative, which giving a contradiction. $\square$

In order to study the types and stabilities of finite equilibria of systems (1), we introduce the Poincaré-Hopf Theorem and the Berlinskii Theorem, see Theorem 6.30 of [21] and Theorem 7 of [19], respectively.

Theorem 5 (Poincaré-Hopf Theorem). *For every tangent vector field on $\mathbb{S}^2$ with a finite number of equilibria, the sum of their topological indices is* 2.

Theorem 6 (Berlinskii Theorem). *Consider the quadratic polynomial differential systems* (2). *Suppose that there are four equilibrium points. If the quadrilateral with vertices at these points is convex then two opposite equilibrium points are saddles and the other two are antisaddles (nodes, foci, or centers). But if the quadrilateral is not convex then either the three exterior vertices are saddles and the interior vertex an antisaddle, or the exterior vertices are antisaddles and the interior vertex a saddle.*

The types and stabilities of the infinite equilibria of systems (1) can be stated as follows:

Proposition 7. *Consider systems* (1) *we have*

  (i) *If $\mu < 0$, then systems* (1) *have two finite equilibria: E_1 is a hyperbolic stable focus, and E_2 is a hyperbolic saddle.*
  (ii) *If $0 \leqslant \mu < 1$, then systems* (1) *have two finite equilibria: E_1 is a hyperbolic stable node, and E_2 is a hyperbolic saddle.*
  (iii) *If $\mu = 1$, then systems* (1) *have two finite equilibria: E_1 is a semi-hyperbolic stable node, and $E_2 = (2,2)$ is a hyperbolic saddle.*
  (iv) *If $\mu > 1$, then systems* (1) *have four finite equilibria: E_1 and E_2 are hyperbolic saddles, E_3 and E_4 are hyperbolic stable foci, see Figure 2.2.*

Proof. First we consider the finite equilibrium $E_1 = (0,0)$. The Jacobian matrix of systems (1) at the equilibrium $E_1 = (0,0)$ is

$$(13) \qquad \begin{pmatrix} -1 & -1 \\ -\mu & -1 \end{pmatrix}.$$

The eigenvalues of the Jacobian matrix (13) are $-1 - \sqrt{\mu}$ and $-1 + \sqrt{\mu}$. It is obvious that E_1 is a hyperbolic saddle when $\mu > 1$, a stable hyperbolic node for $0 \leqslant \mu < 1$, and a hyperbolic stable focus if $\mu < 0$. For the case $\mu = 1$ doing the change of variables $X = x - y, Y = x + y, T = -t$, then systems (1) become

$$(14) \qquad \frac{dX}{dT} = XY, \qquad \frac{dY}{dT} = 2Y - \frac{X^2}{2} - \frac{Y^2}{2}.$$

According to statement (ii) of Theorem 2.19 of [21], we know that the origin of systems (14) is an unstable topological node. Note that we have reverse the time, hence the origin of systems (1) for $\mu = 1$ is a semi-hyperbolic stable node.

Second we study the other finite equilibria. For the case $\mu = 1$, it is obvious that $E_2 = (2,2)$ is a hyperbolic saddle. For the case $\mu < 1$. Since the two infinity equilibria are hyperbolic nodes and the finite equilibrium $E_1 = (0,0)$ is a node

or a focus, the other finite equilibrium E_2 should be a hyperbolic saddle applying Theorem 5 to the Poincaré sphere.

For the case $\mu > 1$. According to Theorem 5 again, the sum of the indices of finite equilibria $E_i, i = 1, 2, 3, 4$ is 0 because the two infinity equilibria are hyperbolic nodes. Thus we can conclude that the quadrilateral with vertices at these finite equilibria is convex by Theorem 6, and then E_2 is a hyperbolic saddle, E_3 and E_4 are hyperbolic antisaddles, i.e. they can be nodes, foci or centers. The equilibria E_3 and E_4 cannot be centers because systems (1) have no periodic orbits by Proposition 4. In the following we prove that E_3 and E_4 are stable foci. The eigenvalues of the Jacobian matrix of systems (1) at a point (x, y) are

$$(15) \qquad\qquad \lambda_{\pm} = -1 \pm \sqrt{(2x - \mu)(2y - 1)}.$$

Let $\mu = 2$, then we know that E_3 and E_4 are stable foci. Since $(2x - \mu)(2y - 1)$ with $\mu > 1$ never vanish in the equilibria E_3 and E_4 of systems (1) and taking into account that the sum of the eigenvalues at any equilibrium point is -2, we can deduce that E_3 and E_4 are stable foci for all $\mu > 1$. $\qquad\square$

3. Proof of Theorem 1

Let $\varphi(t, p)$ be an orbit of an analytic vector field. If this orbit is defined for all $t \geqslant 0$ we denote its $\omega-$limit set as $\omega(p)$ or $\omega(\varphi)$. If this orbit is defined for all $t \leqslant 0$ its $\alpha-$limit set is defined by $\alpha(p)$ or $\alpha(\varphi)$.

Before prove our main result we state the well known Poincaré-Bendixson Theorem and the Markus-Neumann-Peixoto Theorem, see Corollary 1.30 and Theorem 1.43 of [21].

Theorem 8 (Poincaré-Bendixson Theorem). *Let $\varphi(t, p)$ be an integral curve of an analytic vector field $\mathcal{X}$ in $\mathbb{R}^2$ defined for all $t \geqslant 0$, such that $\gamma_p^+ = \{\varphi(t, p) : t \geqslant 0\}$ is contained in a compact set K. Assume that the vector field $\mathcal{X}$ has a finite number of equilibrium points in $\omega(p)$. Then one of the following statement holds.*

(i) *If $\omega(p)$ contains only regular points, then $\omega(p)$ is a limit cycle.*
(ii) *If $\omega(p)$ contains regular and equilibrium points, then $\omega(p)$ is formed by a finite number of orbits $\gamma_1, \gamma_2, \cdots, \gamma_n$ and a finite number of equilibrium points $p_1, p_2, \cdots, p_n$ such that $\alpha(\gamma_i) = p_i, \omega(\gamma_i) = p_{i+1}$ for $i = 1, 2, \cdots, n - 1$, $\alpha(\gamma_n) = p_n$ and $\omega(\gamma_n) = p_1$. Such kind of $\omega-$limit sets are called graphics. Possibly some of the equilibrium points γ_i can be identified.*
(iii) *If $\omega(p)$ does not contain regular points, then $\omega(p)$ is a equilibrium point.*
(iv) *Similar results for the $\alpha-$limit set.*

Let $\mathcal{X}$ be a polynomial vector field, and let $p(\mathcal{X})$ be its Poincaré compactification. Assume that $p(\mathcal{X})$ has finitely many equilibria. Then the set Σ of all separatrices of $p(\mathcal{X})$ in the Poincaré disc are all its infinite orbits, its finite equilibria, its limit cycles and its graphics. It is known that Σ is a closed set in the Poincaré disc $\mathbb{D}^2$. Each open component of $\mathbb{D}^2 \setminus \Sigma$ is called a *canonical region*. Then a *separatrix skeleton* $\mathcal{S}$ of $\mathcal{X}$ or of $p(\mathcal{X})$ is the union of Σ plus an orbit of each canonical region. We say that two separatrix skeletons $\mathcal{S}_1$ and $\mathcal{S}_2$ corresponding to two polynomial vector fields $\mathcal{X}_1$ and $\mathcal{X}_2$ are *equivalent* if there exists a homeomorphism $h : \mathcal{S}_1 \rightarrow \mathcal{S}_2$.

Theorem 9 (Markus-Neumann-Peixoto Theorem). *Assume that $p(\mathcal{X}_1)$ and $p(\mathcal{X}_2)$ are two Poincaré compactifications of two polynomial vector fields $\mathcal{X}_1$ and $\mathcal{X}_2$ with finitely many separatrices. Then their phase portraits in the Poincaré disc are topologically equivalent if and only if their separatrix skeletons are equivalent.*

In order to obtain the position of the local separatrices of the saddle E_1 and E_2 (see Figure 2.2), we introduce the following result which is given in [19].

Lemma 10. *On any straight line which is not composed of paths the total number of equilibrium points and contacts is at most two. If there are two such points, P_1 and P_2, then the paths intersecting the segment ∞P_1 cross in the same sense as the paths intersecting $P_2\infty$ and in the opposite sense to the paths intersecting P_1P_2.*

Proof of Theorem 1. From subsections 2.2 and 2.3, systems (1) have two infinite equilibria, a stable node and an unstable node for all values of $\mu \in \mathbb{R}$. Recall that systems (1) have no periodic orbits and no homoclinic loops by Proposition 4.

(I) For the case $\mu < 0$. There are two finite equilibria: $E_1 = (0,0)$ is a hyperbolic stable focus and E_2 is a hyperbolic saddle by statements (i) of Proposition 7.

Since there are no limit cycles and no graphics, the $\alpha-$ and $\omega-$limit sets of the separatrices of the saddle E_2 it must be equilibrium points by Theorem 8. We know that the two unstable separatrices of the saddle E_2 cannot go together to the stable focus E_1, or to the stable node at infinity, because one of the stable separatrix of the saddle E_2 would not have its $\alpha-$limit set. So one of the unstable separatrices of the saddle E_2 goes to the stable focus E_1 and the other goes to the stable node at infinity. Therefore the two stable separatrices of E_2 have their $\alpha-$limit set at the unstable node at infinity. From the above analysis, the phase portrait of systems (1) for $\mu \geqslant 1$ is topologically equivalent to the one of Figure 1.1.

(II) For the case $\mu \in [0,1]$. There are two finite equilibria: $E_1 = (0,0)$ is a hyperbolic stable node if $\mu \in [0,1)$, or is a semi-hyperbolic stable node if $\mu = 1$, and E_2 is a hyperbolic saddle by statements (ii) and (iii) of Proposition 7. Similar with the proof of case (I) we obtain the phase portrait of systems (1) for $\mu \in [0,1]$ is topologically equivalent to the one of Figure 1.1.

(III) For the case $\mu > 1$. There are four finite equilibria $E_i, i = 1,2,3,4$ by the statement (iv) of Proposition 7, see Figure 2.2. E_i for $i = 1,2$ are hyperbolic saddles, which have two unstable separatrices $s_{i,1}$ and $s_{i,2}$ and two stable separatrices $s_{i,3}$ and $s_{i,4}$. E_i for $i = 3,4$ are hyperbolic stable foci.

We divide the proof of Theorem 1 for $\mu > 1$ into five steps.

Step 1. The flow of systems (1) on the straight line l_1 (see its definition in Figure 2.2) can be determined as follows. According to the orientation of the flow at infinity we can deduce the flows of systems (1) on the segment ∞E_1 is upward, see Figure 2.2. Then we can determine the flow of systems (1) on the segment E_1E_3 and $E_3\infty$ by Lemma 10. The flow of systems (1) on the straight lines l_2, l_4 and l_5 can be deduced similarly. Recall that $l_3 : y = x$. Since the inner product of the vectors $(-1,1)$ and $(y^2 - y - x, x^2 - \mu x - y)$ on the straight line $y = x$ is equal to $(1 - \mu)x$, the flows of systems (1) on the line $y = x$ is described in Figure 2.2.

Thus we can obtain the position of the local separatrices of the saddles E_1 and E_2 as they are indicated in Figure 2.2. Let $\mu = 2$ we know that the finite equilibria E_2 and E_3 are located in the region $y < x$, and E_4 is contained in the region $y > x$. Taking into account the direction of the flows on the straight line l_3 and that the quadrilateral with vertices at these equilibria $E_i, i = 1, 2, 3, 4$ is convex (due to Berlinskii Theorem), then we can deduce that for $\mu > 1$ the equilibria E_2 and E_3 always are located in the region $y < x$, while E_4 is always contained in the region $y > x$.

Step 2. Since systems (1) have no homoclinic loops (see Proposition 4), and taking into account that the sense of the flow of systems (1) on the straight lines l_3 and l_4, we know that the $\alpha-$limit set of separatrix $s_{1,3}$ of the saddle E_1 is the unstable node at infinity. Similarly we can deduce the $\alpha-$limit set of the separatrix $s_{1,4}$ of the saddle E_1 is the unstable node at infinity, and the $\omega-$limit set of the separatrix $s_{2,2}$ of the saddle E_2 is the stable node at infinity.

Step 3. Note that the separatrix $s_{1,4}$ of the saddle E_1 must intersect the straight line l_4 in the segment ∞E_4. It is easy to know using the Poincaré-Bendixson Theorem that the $\omega-$limit set of the separatrix $s_{1,2}$ of the saddle E_1 is the stable focus E_4 because the systems have no periodic orbits (see Proposition 4), and the $\alpha-$limit set of the separatrix $s_{2,3}$ of the saddle E_2 is the unstable node at infinity.

Step 4. We claim using the Poincaré-Bendixson Theorem that the $\omega-$limit set of the separatrix $s_{2,1}$ of the saddle E_2 is the stable focus E_3 because the systems have no periodic orbits (see Proposition 4). Otherwise it can only be the stable node at infinity, this situation cannot occurs because then the $\alpha-$limit set of the separatrix $s_{2,4}$ of the saddle E_2 cannot exist.

Step 5. The remaining separatrices are $s_{1,1}$ and $s_{2,4}$. The $\omega-$limit set of the separatrix $s_{1,1}$ of the saddle E_1 can be either the stable focus E_3 or the stable node at infinity.

Subcase (III.1) If the $\omega-$limit set of the separatrix $s_{1,1}$ of the saddle E_1 is the stable focus E_3, then the $\alpha-$limit set of the separatrix $s_{2,4}$ of the saddle E_2 is the unstable node at infinity. In this case the phase portrait of systems (1) for $\mu > 1$ is topologically equivalent to the one of Figure 1.2. In fact it is not difficult to check that for $\mu > 1$ but close to 1, then the phase portrait of a differential systems (1) is topologically equivalent to Figure 1.2.

Subcase (III.2) If the $\omega-$limit set of the separatrix $s_{1,1}$ of the saddle E_1 is the stable node at infinity, then the $\alpha-$limit set of the separatrix $s_{2,4}$ of the saddle E_2 is also the unstable node at infinity. In this case the phase portrait of systems (1) for $\mu > 1$ is topologically equivalent to the one of Figure 1.3. If $\mu = 20$ it is not difficult to verify that the phase portrait of a differential systems (1) is topologically equivalent to Figure 1.3.

Subcase (III.3) From the above subcases (III.1) and (III.2), we know that the separatrix $s_{1,1}$ of the saddle E_1 and the separatrix $s_{2,4}$ of the saddle E_2 must connect for some value μ^* of the parameter μ by continuity. In this case the phase portrait of a systems (1) is topologically equivalent to the one of Figure 1.4. Moreover, numerically we find that $\mu^* \in (10.4722, 10.4723)$. □

4. Acknowledgements

References

[1] J.C. Artés, J. Llibre, Phase portraits for quadratic systems having a focus and one antisaddle, Rocky Moutain Journal of Mathematics 24 (1994) 875–889.

[2] J.C. Artés, J. Llibre, N. Vulpe, Quadratic systems with a polynomial first integral: A complete classification in the coefficient space $\mathbb{R}^2$, J. Differential Equations 246 (2009) 3535–3558.

[3] J.C. Artés, J. Llibre, N. Vulpe, Quadratic systems with an integrable saddle: A complete classification in the coefficient space $\mathbb{R}^2$, Nonlinear Analysis 75 (2012) 5416–5447.

[4] J.C. Artés, A.C. Rezende, R.D.S. Oliveira, Global phase portraits of quadratic polynomial differential systems with a semi-elemental triple node, Int. J. Bifurcation and Chaos 23 (2013) 1350140-1–21.

[5] C.A. Buzzi, J. Llibre, J.C.R. Medrado, Phase Portraits of Reversible Linear Differential Systems with Cubic Homogeneous Polynomial Nonlinearities Having a Non-degenerate Center at the Origin, Qual. Theory Dyn. Syst. 7 (2009) 369–403.

[6] L. Cairó, J. Llibre, Phase portraits of planar semi-homogeneous vector fields (I), Nonlinear Analysis 29 (1997) 783–811.

[7] L. Cairó, J. Llibre, Phase portraits of planar semi-homogeneous vector fields (II), Nonlinear Analysis 39 (2000) 351–363.

[8] L. Cairó, J. Llibre, Phase Portraits of Planar Semi-Homogeneous Vector Fields (III), Qual. Theory Dyn. Syst. 10 (2011) 203–246.

[9] L. Cairó, J. Llibre, Phase portraits of quadratic polynomial vector fields having a rational first integral of degree 2, Nonlinear Analysis 67 (2007) 327–348.

[10] L. Cairó, J. Llibre, Phase portraits of cubic polynomial vector fields of Lotka-Volterra type having a rational first integral of degree 2, J. Phys. A: Math. Theor. 40 (2007) 6329–6348.

[11] F. Cao, J. Jiang, The Classification on the Global Phase Portraits of Two-dimensional Lotka-Volterra System, J. Dyn. Diff. Equat. 20 (2008) 797–830.

[12] T. Carletti, L. Rosati, G. Villari, Qualitative analysis of the phase portrait for a class of planar vector fields via the comparison method, Nonlinear Analysis 67 (2007) 39–51.

[13] M. Caubergh, J. Llibre, J. Torregrosa, Global phase portraits of some reversible cubic centers with collinear or infinitely many singularities, Int. J. Bifurcation and Chaos 22 (2012) 1250273-1–20.

[14] M. Caubergh, J. Torregrosa, Global phase portraits of some reversible cubic centers with noncollinear singularities, Int. J. Bifurcation and Chaos 23 (2013) 1350161-1–30.

[15] H. Chen, X. Chen, Dynamical analysis of a cubic Liénard system with global parameters, Nonlinearity 28 (2015) 3535–3562.

[16] H. Chen, X. Chen, Dynamical analysis of a cubic Liénard system with global parameters (II)[4], Nonlinearity 29 (2016) 1798–1826.

[17] H. Chen, X. Chen, J. Xie, Global phase portrait of a degenerate Bogdanov-Takens systems with symmetry, Discrete and Continuous Dynamical Systems. Series B 22 (2017) 1273–1293.

[18] B. Coll, A. Ferragut, J. Llibre, Phase portraits of the quadratic systems with a polynomial inverse integrating factor, Int. J. Bifurcation and Chaos 19 (2009) 765–783.

[19] W.A. Coppel, A survey on quadratic systems, J. Differential Equations 2 (1966) 293–304.

[20] F. Dumortier, C. Herssens, Tracing Phase Portraits of Planar Polynomial Vector Fields with Detailed Analysis of the Singularities, Qual. Theo. Dyn. Syst. 1 (1999) 97–131.

[21] F. Dumortier, J. Llibre, J. C. Artés, Qualitative Theory of Planar Differential Systems, Universitext, Spring-Verlag, 2006.

[22] A. Gasull, A. Guillamon, V. Mañosa, Phase portrait of Hamiltonian systems with homogeneous nonlinearities, Nonlinear Analysis 42 (2000) 679–707.

[23] A. Guillamon, C. Pantazi, Phase portraits of separable Hamiltonian systems, Nonlinear Analysis 74 (2011) 4012–4035.

[24] J. Itikawa, J. Llibre, Phase portraits of uniform isochronous quartic centers, Journal of Computational and Applied Mathematics 287 (2015) 98–114.

[25] J. Itikawa, J. Llibre, Global phase portraits of uniform isochronous centers with quadratic homogeneous polynomial nonlinearities, Discrete and Continuous Dynamical Systems. Series B 21 (2016) 121–131.

[26] H. Liang, J. Huang, Y. Zhao, Classification of global phase portraits of planar quartic quasi-homogeneous polynomial differential systems, Nonlinear Dyn. 78 (2014) 1659–1681.

[27] J. Llibre, R.D.S. Oliveira, Phase portraits of quadratic polynomial vector fields having a rational first integral of degree 3, Nonlinear Analysis 70 (2009) 3549–3560.

[28] Y.P. Martínez, C. Vidal, Classification of global phase portraits and bifurcation diagrams of Hamiltonian systems with rational potential, J. Differential Equations 261 (2016) 5923–5948.

[29] R.D.S. Oliveira, A.C. Rezende, Global phase portraits of a SIS model, Applied Mathematics and Computation 219 (2013) 4924–4930.

[30] I. Rajapakse, S. Smale, The Pitchfork Bifurcation, Int. J. Bifurcation and Chaos 27 (2017) 1750132-1-5.

[31] D. Schlomiuk, N. Vulpe, Geometry of quadratic differential systems in the neighborhood of infinity, J. Differential Equations 215 (2005) 357–400.

[32] L. Yang, Recent advances on determining the number of real roots of parametric polynomials, J. Symbolic Computation 28 (1999) 225–242.

[33] C. Zhu, K. Lan, Phase portraits, Hopf bifurcations and limit cycles of Leslie-Gower predator-prey systems with harvesting rates, Discrete and Continuous Dynamical Systems. Series B 14 (2010) 289–306.

[34] C. Zhu, K. Lan, Phase portraits, Hopf bifurcations and limit cycles of the Holling-Tanner models for predator-prey interactions, Nonlinear Analysis: Real World Applications 12 (2011) 1961–1973.

[1] School of Mathematics and Statistics, Guangdong University of Finance and Economics, Guangzhou, 510320, P.R. China

E-mail address: lism1983@126.com

[2] Departament de Matemàtiques, Universitat Autònoma de Barcelona, 08193 Bellaterra, Barcelona, Catalonia, Spain

E-mail address: jllibre@mat.uab.cat